Eves et al., http://www.jcb.org/cgi/content/full/jcb.201201024/DC1

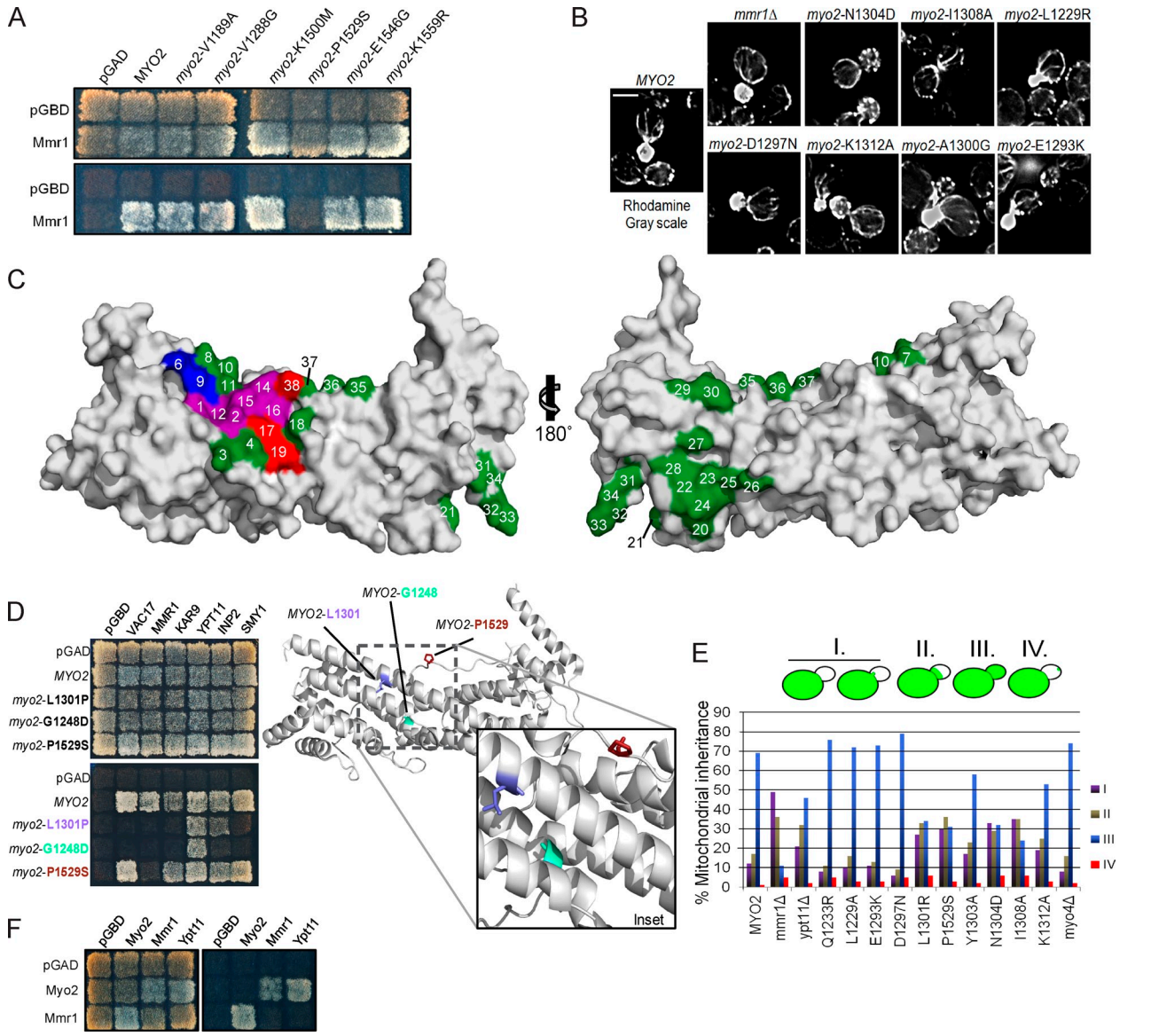

Figure S1. **Surface residues on Myo2 that comprise the Vac17 and Mmr1 binding sites.** (A) *myo2*-P1529S is the sole mutation in *myo2-573* that disrupts Myo2–Mmr1 interactions. (B) Actin cables are not affected in *mmr1Δ* or the myo2 mutants tested. Wild-type, *mmr1Δ*, or *myo2* mutant strains were fixed and stained with phalloidin to visualize filamentous actin. Bar, 5 µm. (C) Surface representation of the crystal structure of the Myo2 CBD. Colored residues indicate residues that were mutated and tested for Mmr1 or Vac17 interaction in a yeast two-hybrid test. Blue: binds Vac17 only; red: binds Mmr1 only; purple: binds Vac17 and Mmr1; green: mutations that did not perturb any of the interactions or phenotypes tested. Residues are indicated as follows: 1, 1,229; 2, 1,233; 3, 1,234; 4, 1,237; 5, 1,248 (*myo2-2*; internal residue); 6, 1,293; 7, 1,295; 8, 1,296; 9, 1,297; 10, 1,299; 11, 1,300; 12, 1,301; 13, 1,302; 14, 1,303; 15, 1,304; 16, 1,307; 17, 1,308; 18, 1,311; 19, 1,312; 20, 1,331; 21, 1,408; 22, 1,411; 23, 1,414; 24, 1,415; 25, 1,418; 26, 1,422; 27, 1,444; 28, 1,447; 29, 1,461; 30, 1,464; 31, 1,480; 32, 1,482; 33, 1,483; 34, 1,484; 35, 1,525; 36, 1,526; 37, 1,528; and 38, 1,529. Note that in the yeast two-hybrid test (Fig. 1), mutation of residues E1299Q and A1300G had a small effect on the interaction with Mmr1. However, the corresponding full-length mutations were not made or tested. (D) Examples of point mutations in Myo2 with defects in binding cargo adaptors that may act by affecting the structure of the Myo2 CBD. (inset) Myo2-G1248 is a buried residue, which is consistent with G1248D affecting the binding of multiple adaptor proteins. Myo2-L1301 and Myo2-P1529 are surface residues. Although L1301 is surface exposed, the side chain is oriented toward helix 4. This likely explains why L1301R and L1301P affect the ability of Myo2 to interact with Vac17 and Mmr1 (Fig. 1 A). To date, P1529S/A solely perturbs Mmr1 binding, which suggests that it is part of the Mmr1-binding region. (E) The *mmr1Δ* mutant exhibits a greater mitochondrial inheritance defect than either *ypt11Δ* or *myo4Δ* mutants. Wild-type (*MYO2*) or the indicated deletion mutant strains were transformed with mitoGFP (*LEU2*) and grown for at least six doubling times before imaging. The absence or presence as well as the position of mitochondria in the bud was scored in small and medium budded cells. Categories I and IV were mutant; categories II and III were wild type–like. $n = 2$; ≥200 cells per strain. (F) Mmr1 and Ypt11 interact with Myo2, but not with each other, in a yeast two-hybrid test. (A, D, and F) Two-hybrid plates incubated at 24°C for 3–4 d. Top left squares in each panel are empty vector controls.

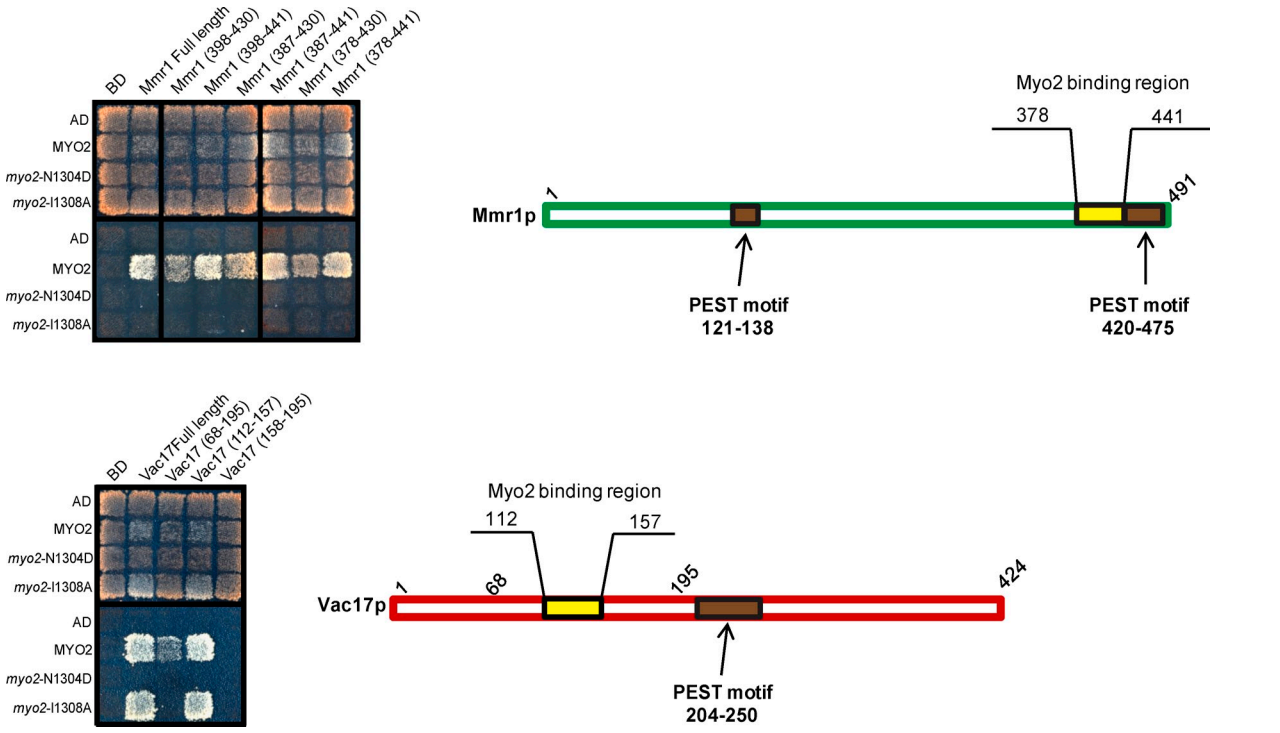

Figure S2. **Mmr1 and Vac17 peptides that bind Myo2 CBD.** Use of two-hybrid analysis to predict peptides of Mmr1 and Vac17 that will interact with Myo2 but not myo2 mutants that are defective in binding Vac17 and Mmr1 in vivo, respectively. Two-hybrid plates incubated at 24°C for 3–5 d. Top left squares in each panel are empty vector controls. The ePEST FIND algorithm on the Mobyle portal (Pasteur Institute) was used for identification of *MMR1* and *VAC17* PEST sequences. AD, activation domain; BD, binding domain.

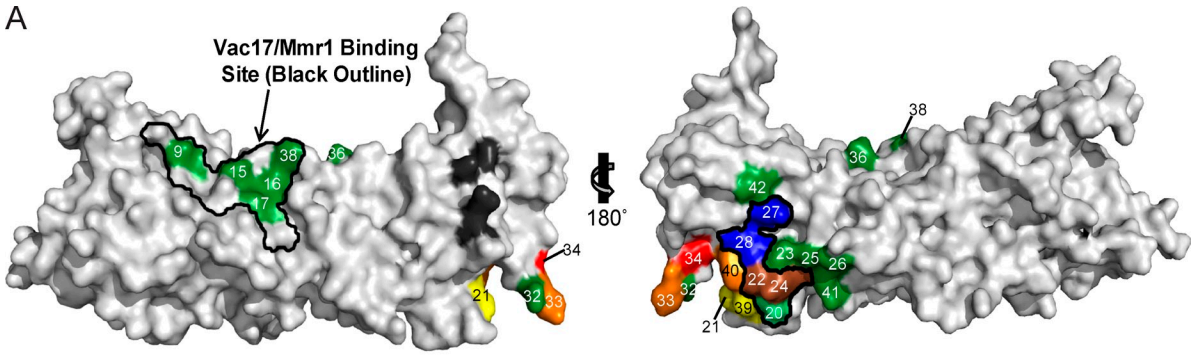

B

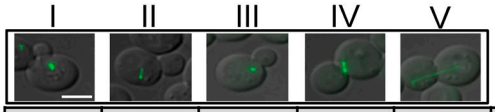

Category:	I		II		III		IV		V		Total	
Allele	*n*	%	*n*	%	*n*	%	*n*	%	*n*	%	***n***	%
MYO2	57	25.6	25	11.2	69	30.9	24	10.8	48	21.5	**223**	100
myo2-G1248D	20	8.5	64	27.2	63	26.8	11	4.7	77	32.8	**235**	100
myo2-N1304D	63	24.7	27	10.6	81	31.8	29	11.4	55	21.6	**255**	100
myo2-L1331S	19	8.8	75	34.9	47	21.9	24	11.2	50	23.3	**215**	100
myo2-F1334A	27	12.5	69	31.9	60	27.8	12	5.6	48	22.2	**216**	100
myo2-W1407F	40	17.7	71	31.4	52	23.0	25	11.1	38	16.8	**226**	100
myo2-K1408A	22	8.9	73	29.7	49	19.9	28	11.4	74	30.1	**246**	100
myo2-L1411R	52	25.4	49	23.9	55	26.8	17	8.3	32	15.6	**205**	100
myo2-N1414S	60	27.6	27	12.4	61	28.1	25	11.5	44	20.3	**217**	100
myo2-Y1415E	38	17.8	68	31.8	39	18.2	26	12.1	43	20.1	**214**	100
myo2-Y1415F	46	20.1	63	27.5	67	29.3	15	6.6	38	16.6	**229**	100
myo2-T1418V	91	33.1	45	16.4	67	24.4	16	5.8	56	20.4	**275**	100
myo2-R1419Q	67	27.9	30	12.5	64	26.7	28	11.7	51	21.3	**240**	100
myo2-K1444A	57	26.3	22	10.1	72	33.2	19	8.8	47	21.7	**217**	100
myo2-Q1447R	54	25.6	22	10.4	63	29.9	27	12.8	45	21.3	**211**	100
myo2-I1462S	78	34.5	41	18.1	55	24.3	13	5.8	39	17.3	**226**	100
myo2-D1482N	61	28.5	30	14.0	66	30.8	14	6.5	43	20.1	**214**	100
myo2-Y1483A	29	12.7	67	29.4	60	26.3	19	8.3	53	23.2	**228**	100
myo2-Y1484A	80	30.1	37	13.9	73	27.4	21	7.9	55	20.7	**266**	100

Figure S3. **Determination of the surface residues on Myo2 that comprise the Rab/Inp2/Kar9 binding sites.** (A) Surface representation of the crystal structure of the Myo2 CBD. Colored residues (except dark green) indicate those sites that when mutated had defects in their ability to interact with any of the Rab GTPases, Kar9, or Inp2. Red: Inp2 only; orange: Kar9 and Inp2; yellow: Kar9 only; green (Myo2-L1331 only): Kar9, Sec4, and Ypt31/32; blue: Sec4, Ypt11, and Ypt31/32; brown: Kar9, Inp2, Sec4, Ypt11, and Ypt31/32. Dark green residues were those tested for Rab GTPases, Kar9, or Inp2 that did not affect binding. These are numbered consistent with Fig. S1 A: 9, 1,297; 15, 1,304; 16, 1,307; 17, 1,308; 20, L1,331; 21, 1,408; 22, 1,411; 23, 1,414; 24, 1,415; 25, 1,418; 26, 1,422; 27, 1,444; 28, 1,447; 31, 1,480; 32, 1,482; 33, 1,483; 34, 1,484; 35, 1,525; 36, 1,526; 38, 1,529; 39, F1,334; 40, W1,407; 41, R1,419; 42, I1,462; and 43, L1,539. (B) Residues that disrupt the Kar9 interaction with Myo2 in a yeast two-hybrid test also disrupted the orientation of spindle microtubules in vivo. Category I: spindle oriented. Category II: spindle misoriented. Category III: microtubules pointed into the focal plane of the image. Category IV: microtubules were near or at the mother–bud neck region. Category V: nuclei were already undergoing separation. Only categories I and II are informative, but all cells were scored, and the results are shown. *n*, number of cells counted from at least two independent experiments. Bar, 5 µm.

References

Catlett, N.L., and L.S. Weisman. 1998. The terminal tail region of a yeast myosin-V mediates its attachment to vacuole membranes and sites of polarized growth. *Proc. Natl. Acad. Sci. USA*. 95:14799–14804. http://dx.doi.org/10.1073/pnas.95.25.14799

Fagarasanu, A., F.D. Mast, B. Knoblach, Y. Jin, M.J. Brunner, M.R. Logan, J.N. Glover, G.A. Eitzen, J.D. Aitchison, L.S. Weisman, and R.A. Rachubinski. 2009. Myosin-driven peroxisome partitioning in *S. cerevisiae*. *J. Cell Biol*. 186:541–554. http://dx.doi.org/10.1083/jcb.200904050

Frederick, R.L., K. Okamoto, and J.M. Shaw. 2008. Multiple pathways influence mitochondrial inheritance in budding yeast. *Genetics*. 178:825–837. http://dx.doi.org/10.1534/genetics.107.083055

Ishikawa, K., N.L. Catlett, J.L. Novak, F. Tang, J.J. Nau, and L.S. Weisman. 2003. Identification of an organelle-specific myosin V receptor. *J. Cell Biol.* 160:887–897. http://dx.doi.org/10.1083/jcb.200210139

James, P., J. Halladay, and E.A. Craig. 1996. Genomic libraries and a host strain designed for highly efficient two-hybrid selection in yeast. *Genetics*. 144:1425–1436.

Jin, Y., P. Taylor Eves, F. Tang, and L.S. Weisman. 2009. PTC1 is required for vacuole inheritance and promotes the association of the myosin-V vacuole-specific receptor complex. *Mol. Biol. Cell*. 20:1312–1323. http://dx.doi.org/10.1091/mbc.E08-09-0954

Pashkova, N., N.L. Catlett, J.L. Novak, and L.S. Weisman. 2005. A point mutation in the cargo-binding domain of myosin V affects its interaction with multiple cargoes. *Eukaryot. Cell*. 4:787–798. http://dx.doi.org/10.1128/EC.4.4.787-798.2005

Pashkova, N., Y. Jin, S. Ramaswamy, and L.S. Weisman. 2006. Structural basis for myosin V discrimination between distinct cargoes. *EMBO J.* 25:693–700. http://dx.doi.org/10.1038/sj.emboj.7600965

Sheffield, P., S. Garrard, and Z. Derewenda. 1999. Overcoming expression and purification problems of RhoGDI using a family of "parallel" expression vectors. *Protein Expr. Purif*. 15:34–39. http://dx.doi.org/10.1006/prep.1998.1003

Sikorski, R.S., and P. Hieter. 1989. A system of shuttle vectors and yeast host strains designed for efficient manipulation of DNA in *Saccharomyces cerevisiae*. *Genetics*. 122:19–27.

Song, S., and K.S. Lee. 2001. A novel function of *Saccharomyces cerevisiae* CDC5 in cytokinesis. *J. Cell Biol*. 152:451–469. http://dx.doi.org/10.1083/jcb.152.3.451

Tang, F., E.J. Kauffman, J.L. Novak, J.J. Nau, N.L. Catlett, and L.S. Weisman. 2003. Regulated degradation of a class V myosin receptor directs movement of the yeast vacuole. *Nature*. 422:87–92. http://dx.doi.org/10.1038/nature01453

Table S1 shows yeast strains used in this study and is provided as an Excel file.

Table S2 shows plasmids used in this study and is provided as an Excel file.

Table S3 shows a summary of yeast two-hybrid and in vivo analyses and is provided as an Excel file.